FTIR Investigation of the H_2, N_2, and C_2H_4 Molecular Complexes Formed on the Cr(II) Sites in the Phillips Catalyst: a Preliminary Step in the understanding of a Complex System

E. Groppo,* C. Lamberti, S. Bordiga, G. Spoto, A. Damin, and A. Zecchina

Department of Inorganic, Physical and Materials Chemistry, and NIS center of excellence, University of Torino, via P. Giuria 7, I-10125 Torino, Italy

Received: April 8, 2005; In Final Form: May 23, 2005

This work reports the first complete FTIR characterization of H_2, N_2 and C_2H_4 molecular complexes formed on the Cr(II) sites in the Phillips catalyst. The use of a silica aerogel as support for Cr(II) sites, substituting the conventional aerosil material, allowed us to obtain a remarkable increase in the signal-to-noise ratio of the IR spectra of adsorbed species. The improvement is directly related to an increase of the surface area of the support ($\sim$700 m^2g^{-1}) and to an almost complete absence of scattering [Groppo et al., *Chem. Mater*. **2005**, *17*, 2019−2027]. The use of this support and the adoption of suitable experimental conditions results, for the first time, in the clear observation of H_2 and N_2 adducts formed on two different types of Cr(II) sites, thus yielding important information on the coordinative state of the Cr(II) ions, which well agrees with the evidences provided in the past by other probe molecules. Furthermore, we report the first complete characterization of the C_2H_4 π-complexes formed on Cr(II) sites. These results are particularly important in the view of the understanding of the polymerization mechanism, since the C_2H_4 coordination and the formation of π-bonded complexes are the first steps of the reaction.

1. Introduction

Nowadays, more than one-third of all the polyethylene produced in the world is obtained by means of the Cr/SiO_2 Phillips catalyst.[1−3] This system is easily obtained by grafting Cr(VI) ions on the surface of an amorphous silica support and then contacting it directly with ethylene at about 400 K. After a short induction period, during which Cr(VI) is reduced to Cr(II), the polymerization takes place.[4] Due to the morphology of the structure, different locations of Cr(II) on the surface are possible, a fact which makes the characterization effort a complex and difficult task. For this reason, despite the numerous investigations since its discovery, two main questions still remain unresolved, i.e., the structure of the really active sites and the polymerization mechanism.[1] Quite paradoxically, if the heterogeneity of the system is making the understanding of the surface sites structure quite elusive, at the same time it is at the origin of its success, since the exploitation of many types of active sites allows to produce many types of polymers. To try to make light on these open questions, a simplified version of the catalyst has been used since the beginnings of research in this field, obtained by reduction of the surface chromate precursors with CO at 623 K.[1,4,5] In this way, the oxidation state of Cr is well defined, mainly Cr(II), and the reduction and the polymerization phases are well separated.

The structure of the Cr(II) species has been widely investigated by several spectroscopic techniques, among which UV−vis DRS,[1,6−9] FTIR,[1,10−23] Raman,[1,9,24−26] XAS,[1,8,27,28] and XPS.[1,29,30] In particular, FTIR spectroscopy of adsorbed probe molecules has been largely used in the past to infer the nuclearity and the oxidation state of the Cr(II) adsorption sites on the Phillips catalyst, as well as their coordination environment. CO and NO molecules have been by far the most used and the most informative,[6,10−15,21,23] but also CO_2, N_2O, and pyridine adsorption has been reported.[7,16] The analysis of all these results leads to a very complex and heterogeneous scenario, which reflects the high heterogeneity of the silica support.[1] Different types of Cr(II) sites have been classified, according to their coordinative unsaturation and thus to their ability to form different molecular adducts with probe molecules. At room temperature, Cr(II) sites have been found to coordinate up to two molecules of CO, NO, CO_2, and N_2O, while lowering the temperature down to 77 K further ligands can be inserted from the gas phase. The insertion of molecules from the gas phase is often accompanied by the displacement of weaker ligands such as the siloxane groups present on the dehydroxilated silica surface. According to the nomenclature adopted in refs 1, 11, 13, 15, 21, 23, 31, and 32, we can basically distinguish two families of Cr(II) ions: Cr^{II}_B sites (able to coordinate only one CO molecule at RT) and Cr^{II}_A sites (able to coordinate up to 2 CO molecules at RT). These species are characterized by a different polarizing ability (greater for Cr^{II}_B) and by a different propensity to give d-π back-donation (greater for Cr^{II}_A). It is also well-known that a thermal treatment in vacuum at high temperatures modifies the relative population of the Cr centers, favoring the sinking of the less coordinatively saturated sites (Cr^{II}_A) into the flexible surface of the amorphous silica.[1,21]

The use of H_2 and N_2 as probe molecules for supported transition metal sites is less common than that of CO and NO, and has not been yet reported in the case of the Cr/SiO_2 system. This is due, first of all, to the wide spread conviction that IR inactive molecules are less useful for probing the surface sites structures than CO and NO, because the intensity of the bands resulting from the activation of their stretching modes is

* Corresponding author. Tel.: +39011-6707840. Fax: +39011-6707855. E-mail: elena.groppo@unito.it.

10.1021/jp051826w CCC: $30.25
Published on Web 07/15/2005

expected to be lower. This is particularly true when the interaction is weak. IR manifestation of the adsorbed species can represent a critical limitation in the case of catalysts such as Cr/SiO_2. The very low concentration of Cr sites present on the silica surface (a typical catalyst contains about 0.5−1.0 wt % Cr, corresponding to about 0.2−0.4 Cr atoms per nm^2, for a standard silica having a surface area of 400 m^2g^{-1}) requires in fact a high sensitivity in order to observe the manifestation of the molecular complexes with a reasonable signal-to-noise ratio. This last point has prevented so far also a systematic investigation of the $Cr(II)\cdots C_2H_4$ complexes, which are the precursor species for the ethylene polymerization. The observation of these molecular adducts is further on hampered by the very high polymerization activity of the Phillips catalyst. At RT, in fact, the ethylene polymerization starts almost immediately and with a very high turnover frequency, so that the possibility to detect precursor and intermediate species is necessarily related with the adoption of special experimental strategies.[1,33]

In this work we report the observation, by means of FTIR spectroscopy, of H_2 (D_2), N_2 and C_2H_4 (C_2D_4) molecular adducts on the Cr(II) sites on the Phillips catalyst. The aim of the study is two-fold: (i) to improve the knowledge about the structure of the Cr(II) sites by a direct comparison with the results obtained in the past by means of other probe molecules (mainly CO); (ii) to clarify the nature of the C_2H_4 adducts with Cr(II) sites, which is the first logical step in the identification of the polymerization mechanism for the Phillips catalyst. To increase the number of Cr(II) sites probed by these molecules, and thus to improve the signal-to-noise ratio of our spectra, we have used as support material a silica-aerogel.[26] This support is chemically equivalent to a standard aerosil, as testified by FTIR spectroscopy which shows OH and SiO stretching bands comparable to those observed in the case of a silica-aerosil, but possesses a much higher surface area than that of the commonly used amorphous aerosil (from ∼380 to ∼700 m^2g^{-1}). Furthermore, it is characterized by a scattering considerably smaller: this allows to work in transmission mode with very thick pellets, thus increasing the number of Cr sites detected by the IR beam along the path (and hence the sensitivity). The use of Cr/aerogel system is also justified by the observation that ethylene polymerization performed on both supports under comparable conditions basically reflects a similar catalytic activity for the two systems.[1] It will be shown that the use of this support and the adoption of suitable experimental conditions allows to clearly observe, for the first time, H_2 and N_2 complexes formed on two different types of Cr(II) sites, thus yielding important information on the coordinative state of the Cr(II) ions, which well agrees with the evidences provided by other probe molecules. Furthermore, we report the first complete characterization of the C_2H_4 complexes formed on Cr(II) sites. These results are particular important in the view of the understanding of the polymerization mechanism, since the C_2H_4 coordination and the formation of π-bonded complexes are the first steps of the reaction.

2. Experimental Section

The $Cr(II)/SiO_2$ samples (1 wt % Cr) have been prepared by impregnating silica-aerogel monolites with a solution of CrO_3 in CH_3CN. The aerogel monolites were kindly supplied by Novara Technology[34] and present a surface area of about 700 m^2g^{-1}. The impregnated monolites were then dried at RT, reduced in powder and pressed into a thick pellet (∼0.5 mm). Even after grinding, the silica-aerogel guarantees an almost complete transparency of the sample in the IR region in the 4500−1800 cm^{-1} range (vide infra Figure 3), because of the absence of scattering. The pellet has been then transferred into an IR cell designed to allow thermal treatments of the sample in the 1000−77 K range, either under vacuum or in the presence of a desired equilibrium pressure of gases. The samples were activated according to the following procedure: (i) activation at 923 K; (ii) calcination in O_2 at the same temperature for 1 h; (iii) reduction in CO at 623 K, followed by CO removal at the same temperature; (iv) cooling to RT. The FTIR spectra have been collected on a Bruker IFS-66 spectrophotometer, at 2 cm^{-1} resolution.

3. Results and Discussion

3.1. H_2 Molecular Adducts. It is known that H_2 can interact with a variety of systems such as (i) bare cations,[35−37] (ii) coordinatively unsaturated cationic centers or cation/anion pairs at the surface of ionic solids,[38,39] (iii) Brønsted and Lewis sites in protonic or cation exchanged zeolites and zeotypes,[40−43] and (iv) metalorganic frameworks[44] through molecular (with formation of surface dihydrogen adducts) or dissociative (heterolytic splitting of the H_2 molecule) adsorption paths. Both the interaction mechanisms can be conveniently investigated by IR spectroscopy. In fact, although the ν(HH) stretching mode is IR inactive in the gas phase, it gains activity when the H_2 molecule is polarized upon non dissociative adsorption and shifts to lower wavenumbers as compared to the 4161 cm^{-1} Raman frequency in the free state. For weak perturbation, as is for instance the case of molecular adducts involving non-d cations where electrostatic forces are mainly operating, the shift $\Delta\tilde{\nu}$(HH) is roughly proportional to the adsorption energy and highly sensitive (as compared to other diatomic probes such as CO or NO) to surface heterogeneity (in terms of polarizing power and structure of the adsorbing sites).[39,40,43,45] When transition metal centers are involved, the $M^+\cdots H_2$ binding energy and the $\Delta\tilde{\nu}$(HH) shift are influenced by several factors such as the cost of hybridization, the metal−ligand repulsion and the extent of charge transfer beside the interaction between the cationic charge and the induced dipole and quadrupole moments of the adsorbed H_2 molecule. In other words, the $M^+\cdots H_2$ interaction results to be highly sensitive to the electronic structure as well as to the coordinative state of the cation.[35,46,47] As said before, IR spectroscopy has proved its utility also when dissociative adsorption is occurring, as on MgO, where Mg^{2+}-H^- hydrides and hydroxilic species are formed characterized by well defined, structure sensitive IR peaks.[39]

Going to the interaction of H_2 with the $Cr(II)/SiO_2$ system, neither molecular nor dissociative adsorption have been reported in previous studies at 273 K on the conventional (aereosil based) catalyst. On the contrary, upon H_2 dosage at 77 K on our aereogel based samples, characterized by little scattering of the IR radiation in the high-frequency region (>3000 cm^{-1}), the appearance of weak bands covering the whole 4450−3900 cm^{-1} region and reversible upon outgassing at the same temperature can be appreciated (as shown in Figure 1). Since these bands are absent when H_2 is dosed at 77 K on the bare SiO_2 (spectra not reported for brevity) and on the basis of the literature quoted at the beginning of this paragraph, these bands can be safely assigned to the formation of $Cr(II)\cdots H_2$ molecular adducts. More in detail, the manifestations in Figure 1 can be assigned[39,43,48] to (i) the fundamental ν(HH) vibration of adsorbed H_2 (bands in the 3975−3900 cm^{-1} range), (ii) $\nu(HH)+\nu(Cr-H_2)$ combination modes involving the H−H stretching and the motion of the molecules against the adsorption center or, more in general, frustrated translational motions (bands in the 4300−4100 cm^{-1}

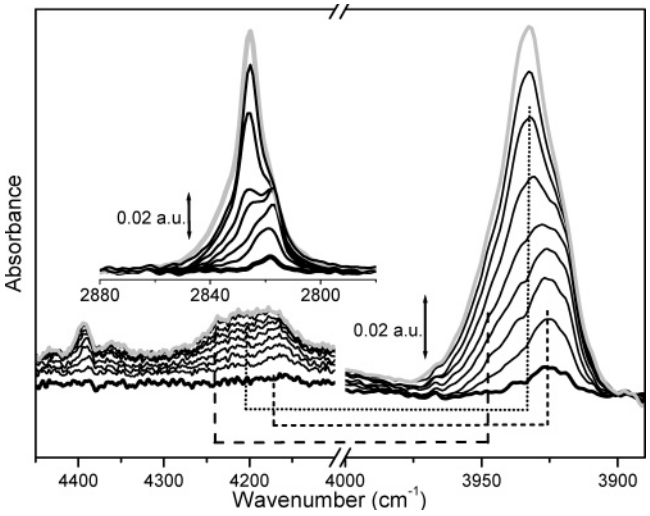

Figure 1. Background subtracted FTIR spectra of H_2 adsorbed on $Cr(II)/SiO_2$-aerogel at 77 K at increasing equilibrium pressures (from bold black to gray curves). The manifestations in the 4000−3900 cm^{-1} interval are due to the pure vibrational $\tilde{\nu}$(HH) modes of $Cr(II)\cdots H_2$ molecular adducts, while those in the 4450−4100 cm^{-1} region are due to combination and rotovibrational modes of the same species (dotted and dashed lines show the correspondence between the two frequency intervals). The assignment of the bands in the 4000−3900 cm^{-1} region is schematized in Scheme 1. The inset reports the pure vibrational $\tilde{\nu}$(DD) modes of $Cr(II)\cdots D_2$ molecular adducts formed in the same experimental conditions.

SCHEME 1

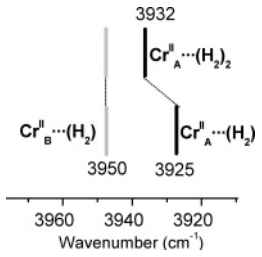

region), and (iii) vibrational−rotational components (band at about 4400 cm^{-1}) which testify that the adsorbed molecules still possess some (hindered) rotational freedom.

A closer inspection of Figure 1 reveals that the absorption in 3975−3900 cm^{-1} region is characterized by the superposition of at least three components, behaving in different ways upon changes of the H_2 equilibrium pressure (see Scheme 1). The spectra at low-medium pressures show in fact the growth of a band at about 3925 cm^{-1} ($\Delta\tilde{\nu}$(HH) = −236 cm^{-1}), with a high-frequency broad tail at ca. 3950 cm^{-1} ($\Delta\tilde{\nu}$(HH) = −211 cm^{-1}). Upon increasing the H_2 pressure, the intensity of the band at 3925 cm^{-1} reaches a maximum and then declines, while a new component simultaneously develops at 3932 cm^{-1} ($\Delta\tilde{\nu}$(HH) = −229 cm^{-1}), which finally dominates the spectrum. In the investigated pressure range the monotonic increase of the shoulder at 3950 cm^{-1} is finally observed upon increasing the H_2 pressure. The presence of three distinct components is even more evident in the spectra obtained upon dosage of D_2 instead of H_2 (inset in Figure 1): the maxima are now at 2819 cm^{-1} (derived from the 3925 cm^{-1} band in H_2), 2835 cm^{-1} (3950 cm^{-1} in H_2), and 2826 cm^{-1} (3932 cm^{-1}) (notice that in all cases the $\tilde{\nu}(H_2)/\tilde{\nu}(D_2)$ isotopic shift is 1.39). To account for the fact that the different components look better resolved in the D_2 case with respect to H_2 it is useful to recall that natural hydrogen is the mixture of two species differing for the total nuclear spin I: *para*- ($I = 0$) and *ortho*-hydrogen ($I = 1$) (with an *o*/*p* natural abundance = 3). The two isomers have slightly different vibrational frequencies in the free state (4161.1 cm^{-1} for *p*-H_2 and 4155.2 cm^{-1} for *o*-H_2, resulting in a split of 6 cm^{-1}) as well as in the adsorbed state.[49,50] *Ortho-para* splitting is therefore expected to contribute (together with surface heterogeneity) to the broadening of the adsorption bands of the $Cr(II)\cdots H_2$ adducts. In the D_2 case, the splitting in the gas phase is 2 cm^{-1} only and the contribution to broadening consequently negligible: this is clearly reflected in the spectra of Figure 1, where the fwhm (full width at half maximum) measured on the most intense curves results to be 31 cm^{-1} for the H_2 molecular adducts and only 16 cm^{-1} for the corresponding deuterated species.

As far as the detailed assignment of the 3950, 3932, and 3925 cm^{-1} triplet is concerned, we attribute the 3950 and 3925 cm^{-1} bands to $Cr(II)\cdots H_2$ adducts containing a single H_2 ligand in the coordination sphere but formed on two structurally different Cr sites (see Scheme 1). As the band at 3925 cm^{-1} is the first to appear already at very low equilibrium pressure and is characterized by a larger downward shift of ν(HH) mode, it is assigned to H_2 adsorbed on Cr(II) sites characterized by a higher coordinative unsaturation as compared to those responsible for the 3950 cm^{-1} absorption. The existence of two different Cr sites is well ascertained by previous works and, according to the nomenclature adopted in the literature concerning the interaction of CO with the $Cr(II)/SiO_2$ system,[1,11,13,15,21,23,31,32] the 3925 and 3950 cm^{-1} bands are therefore ascribed to $Cr^{II}_A\cdots H_2$ (3925 cm^{-1}) and $Cr^{II}_B\cdots H_2$ (3950 cm^{-1}) adducts, respectively. On the basis of the existent literature of H_2 complexes on cationic centers,[51−53] we suggest that H_2 adsorbs on Cr(II) sites in a side on geometry. Conversely, the formation of complexes involving both the Cr(II) site and the neighboring oxygen anions[54,55] seems less probable, due to the negligible basic character of the oxigens anions on the silica surface. The spectral behavior upon pressure increase can be interpreted in terms of the addition of a second H_2 molecule on Cr^{II}_A sites resulting in the formation of $Cr^{II}_A\cdots(H_2)_2$ adducts (see Scheme 1). The parallel experiment with D_2 supports this assignment. The adsorption capability at 77 K of the two families of sites toward H_2 (D_2) mirrors perfectly what already observed at RT by dosing CO.

The frequency shifts which characterize the $Cr(II)\cdots H_2$ molecular adducts with respect to the gas phase, $\Delta\tilde{\nu}$(HH) = −236 and −211 cm^{-1}, deserves a comment. In particular, a comparison with the shifts observed for H_2 interacting with other cations is of particular utility. $\Delta\tilde{\nu}$(HH) values as high as −1031 and −1082 cm^{-1} have been recently reported in the case of $Cu(I)\cdots H_2$ adducts on two different Cu(I) sites hosted inside the channels of ZSM-5 zeolite.[47] This impressive shift is explained in terms of the presence of an extensive covalent metal−hydrogen interaction, involving a strong chemical contribution (donation from the H_2 σ orbital and back-donation from the 3dπ Cu(I) orbitals).[47,56] A much lower shift, $\Delta\tilde{\nu}$(HH) = −60 cm^{-1}, has been conversely reported in the case of $Na^+\cdots H_2$ adducts formed in the analogous Na^+-ZSM-5 system, where electrostatic polarization effects are dominating and the σ donation/dπ back-donation contributions are absent.[47,54] The $\Delta\tilde{\nu}$(HH) = −236 (−229) cm^{-1} found here for the $Cr(II)\cdots H_2$ adducts suggests that some covalent character is present, even if the interaction is less strong than in the case of $Cu(I)\cdots H_2$ adducts, the latter being visible also at RT. The covalent character of the $Cr(II)\cdots H_2$ bonds also accounts for the low intensity of the $\tilde{\nu}$(HH) mode because, as observed for $Cu(I)\cdots H_2$

adducts, the H−H stretching is not accompanied by strong dipole oscillations along the covalent Cr(II)−H and H−H bonds.

Coming to the 4450−4100 cm^{-1} interval of the spectra reported in Figure 1, a complex absorption centered at about 4200 cm^{-1} and a much narrower band at 4394 cm^{-1} are clearly evident. On the basis of the existing literature,[39,40] we assign the broad absorption at about 4200 cm^{-1} to the combination of the ν(HH) stretching mode with the frustrated translational modes of the H_2 molecule along the direction perpendicular to the surface, $\nu(Cr-H_2)$. The evolution of these absorptions upon increasing the H_2 equilibrium pressure mirrors that already discussed for the pure vibrational ν(HH) components (3975−3900 cm^{-1} region), so that correspondences between the two groups of bands can be inferred (see dotted and dashed lines in Figure 1). Conversely, the assignment of the band at 4394 cm^{-1}, surely associated with a rotovibrational mode, is not straightforward. The rotovibrational components for *ortho* and *para*-H_2 in the gas phase occur at $\tilde{\nu} = \tilde{\nu}(HH) + 600$ cm^{-1} and at $\tilde{\nu} = \tilde{\nu}(HH) + 360$ cm^{-1}, respectively. The band at 4394 cm^{-1}, which appears at high H_2 pressures and occurs at $\tilde{\nu} = \tilde{\nu}(HH) + 460$ cm^{-1}, could be the rotovibrational manifestation of *orto*-H_2 adsorbed on Cr^{II}_A sites, strongly perturbed with respect to the gas phase.

Finally, it is worth underlining that, under the experimental conditions of the spectra reported in Figure 1 (77 K), the Si−OH band at 3746 cm^{-1} (spectral region not reported in the figure for brevity) is not perturbed at all. The possibility of an interaction of H_2 with the silanols group present on the silica surface must be therefore ruled out. Furthermore, the absence of IR bands in the low frequency region, where a chromium-hydride species are expected to absorb, testifies that only Cr(II)···H_2 molecular adducts are formed and that no splitting reaction occurs on the Cr(II) sites. This observation is particularly important, because the dissociative chemisorption of H_2 at the active Cr(II) sites or at strained siloxane defects has been claimed to be responsible of the activation of suitably positioned Cr(II) sites, thus explaining the acceleration of ethylene polymerization in the presence of H_2 (which is opposite to the catalytic activity depression generally observed in the presence of H_2 for the Ziegler−Natta and chromocene catalysts).[57]

3.2. N_2 Molecular Adducts. Unlike H_2, N_2 is adsorbed on the Cr(II)/SiO_2-aerogel system already at RT (although weakly), as demonstrated by the appearance in the IR spectrum of a narrow band at 2328 cm^{-1} (accompanied by a weak shoulder at about 2333 cm^{-1}) and by a weaker component at 2337 cm^{-1} (gray curve in Figure 2). The same bands, with enhanced intensity and a different intensity ratio, have been recently observed also by means of Raman spectroscopy.[26,28] It is worth noticing that, despite the relatively large number of known coordination complexes with transition metals containing N_2 as a ligand,[58,59] only a few examples of N_2 complexes formed on oxides surfaces[60,61] or on metal exchanged zeolites[45,62−68] have been reported, most of them formed in low temperature and/or high-pressure conditions. The finding that N_2 is already adsorbed at RT on Cr/SiO_2 merits therefore a special attention.

Opposite to the H_2 case, the end-on geometry is largely predominant in dinitrogen coordination compounds[58,59] or in dinitrogen-transition metal adducts in supported systems,[45,64−66] and the side-on one is very rarely encountered. Upon coordination to vacant sites of metal centers, the stretching frequency of N_2 can undergo downward or upward shifts. Dinitrogen coordinated to transition metal centers (e.g. Fe^{2+}, Co^{+}, Ru^{2+}, Re^{+}, Os^{2+} etc.) in mononuclear and binuclear homogeneous

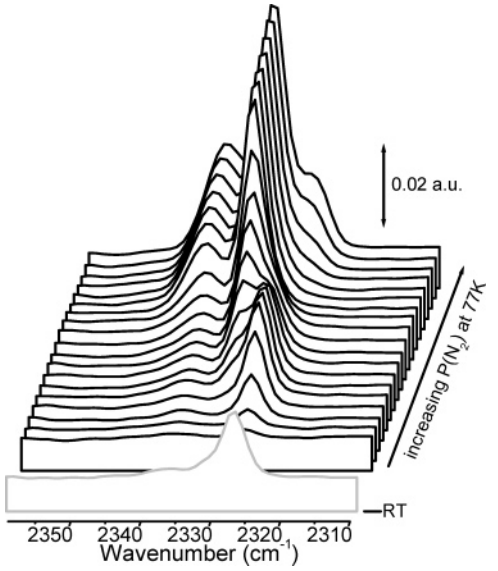

Figure 2. Background subtracted FTIR spectra of N_2 adsorbed on the Cr(II)/SiO_2-aerogel catalyst. Gray curve: 30 Torr of N_2 at RT. Black curves: increasing the N_2 pressures at 77 K. The proposed assignment of the bands in the 2350−2310 cm^{-1} region is reported in Scheme 2.

complexes usually exhibits the $\tilde{\nu}$(NN) band in the 2200−1700 cm^{-1} region,[59] i.e., with a $\Delta\tilde{\nu}$(NN) in the range between −131 and −631 cm^{-1}, with respect to the Raman frequency of unperturbed N_2 (2331 cm^{-1}). Such large negative shifts are explained in terms of a synergic σ-donor/π-acceptor interaction, both ligand-to-metal σ-donation and metal-to-ligand π-back-donation contributing to weaken the N≡N bond. Donation/back-donation effects are also operating in the case of the Cu(I)···N_2 adducts formed inside the Cu(I)−ZSM-5 zeolite, although the shift, $\Delta\tilde{\nu}(NN) = -36$ cm^{-1}, is definitely smaller.[62,64,66,67] Conversely, the interaction of N_2 with non transition metal ions, where electrostatic effects are absolutely predominating, causes an increase of the $\tilde{\nu}$(NN) mode, which reaches a maximum [$\Delta\tilde{\nu}(NN) = +10$ cm^{-1}] for Li-exchanged mordenite.[65] The very small $\Delta\tilde{\nu}$(NN) observed here for the Cr(II)···N_2 adducts (−3 and +6 cm^{-1} for the two bands, respectively), suggests a balancing of the positive shift induced by the electrostatic interaction and the opposite effect due to $\sigma-\pi$ interaction. The resulting bond is however sufficiently strong to justify the observation of Cr(II)···N_2 adducts even at RT and the sample change of color from blue-green to light blue upon N_2 adsorption.[26] Note that in order to observe the formation of M^+···N_2 adducts inside zeolitic frameworks ($M^+ = Li^+$, Na^+, K^+, and Cs^+) liquid nitrogen temperatures are required.[45,65]

When the N_2 coverage at the surface is gradually increased (increasing equilibrium pressures at 77 K), the FTIR spectrum is modified as follows (Figure 2, black curves): (i) the band at 2328 cm^{-1} grows up to a saturation point and then progressively disappears, with the simultaneous formation of a new intense component at 2333 cm^{-1}; (ii) the band at 2337 cm^{-1} only grows in intensity and slightly shifts to 2340 cm^{-1}. Analogously to the H_2 case (even if the adducts geometry is not the same, end-on for N_2 adducts vs side-on for H_2 ones), the evolution of the 2328 cm^{-1} band in the 2333 cm^{-1} one may be interpreted in terms of addition of a second N_2 molecule to the first formed Cr(II)···N_2 complex (responsible of the band at 2328 cm^{-1}). Based on the literature data concerning homogeneous dinitrogen complexes[58,59] and transition-metals-dinitrogen adducts isolated in low-temperature matrixes,[69,70] a coupling between the two N_2 oscillators, which should cause a splitting of the $\tilde{\nu}$(NN) band, seems less probable. Following the nomenclature given in the

SCHEME 2

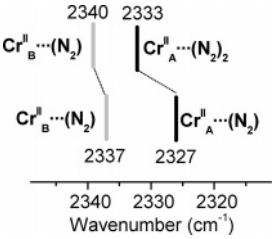

case of CO adsorption and remembering that N_2 is a weaker ligand, it is conceivable that, at RT, only one N_2 molecule may adsorb both on Cr^{II}_A and Cr^{II}_B sites. The peak at 2328 cm^{-1} ($\Delta\tilde{\nu} = -3$ cm^{-1}) may be assigned to the N_2 adsorbed on the Cr^{II}_A sites, while the band at 2337 cm^{-1} ($\Delta\tilde{\nu} = +6$ cm^{-1}) may be due to the N_2 adsorbed on the Cr^{II}_B sites, characterized by a higher polarization ability and/or a less tendency to give d-π interactions with respect to the Cr^{II}_A centers (see Scheme 2). At higher pressure (lower temperature) a second N_2 molecule is able to insert into the $Cr^{II}_A\cdots N_2$ complex, giving rise to the band at 2333 cm^{-1}, while Cr^{II}_B sites remain able to coordinate only one N_2 molecule.

Finally it is worth noticing that, at the highest N_2 pressures, a new broader absorption develops at ca. 2325 cm^{-1}. The formation of this band is accompanied, in the OH region, by the partial erosion of the silanols band at 3746 cm^{-1} and the growth of a new weak band at 3725 cm^{-1} (not shown for clarity). These are the spectroscopic manifestation of the interaction of N_2 with the silanols groups of the silica surface that begin to be appreciable only at liquid nitrogen temperatures and at high-pressure values.

3.3. C_2H_4 π-Bonded Complexes. At RT C_2H_4 cannot be considered as a proper probe molecule for the Cr(II) sites in the Phillips catalyst, since its coordination is followed by a very fast polymerization reaction. It is consequently clear that the study of the Cr(II)$\cdots C_2H_4$ complexes can be achieved only upon lowering the temperature down to a value where kT is lower than the activation barrier of the first step of the polymerization reaction.[33] Only under such experimental conditions the Cr(II)$\cdots(C_2H_4)_n$ species may be observed, so giving the possibility to elucidate the coordination state of the Cr(II) sites (like H_2 and N_2) and, hopefully, to have an insight into the first steps of the polymerization mechanism. The interaction of olefins with organometallic compounds and metal surfaces has been extensively studied in the past. The metal-olefin π-bond is in general described following the mechanism of Chatt-Dewar-Ducanson,[71] involving electron donation from the olefin π molecular orbital to the metal d empty orbital and electron back-donation from the metal to the olefin π^* molecular orbital. The vibrational spectroscopy of metal-bonded olefins has produced an abundant literature concerning metals-olefins systems in low-temperature matrixes, in which the metals are in zerovalent state.[72−74] Conversely, only few vibrational data are present in the literature concerning the interaction of olefins with charged metal species.[75−77]

In the past several attempts have been performed in order to identify the species formed in the very initial steps of the ethylene polymerization reaction on the Cr(II)/SiO_2 system by means of FTIR spectroscopy.[1,15,23,78,79] By decreasing the ethylene polymerization rate several authors reported the appearance, in the first stages of the reaction, of few bands assigned to Cr(II)$\cdots C_2H_4$ complexes.[15,78,79] However, in these conditions the monomer concentration rapidly decreases and the vibrational features of the polymeric products overcome

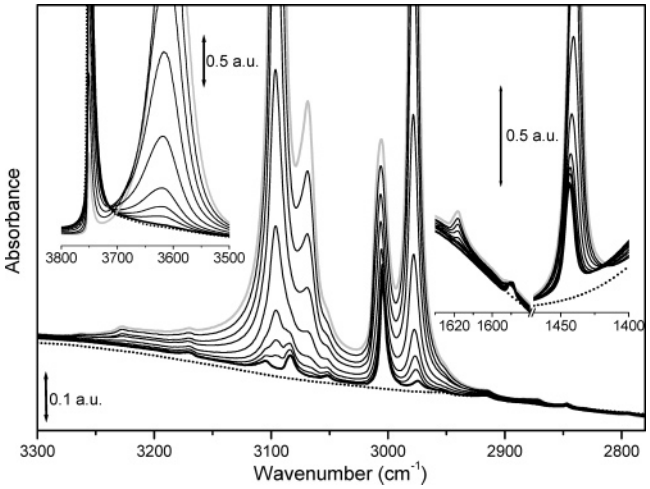

Figure 3. Temperature resolved FTIR spectra of the C_2H_4 adsorption on the Cr(II)/SiO_2-aerogel catalyst in the 120−230 K range. The CH_2 stretching (central part), OH stretching (left inset), and C=C stretching and CH bending (right inset) regions are illustrated separately. Dotted curve: Cr(II)/SiO_2-aerogel sample before contact with ethylene. Gray curve: C_2H_4 interaction at 120 K. Black curves: C_2H_4 interaction at progressively increasing T, up to 230 K, bold black curve. In the heating ramp (evolution form gray to bold black curve) all components decrease in intensity except for the band at 3746 cm^{-1} due to the unperturbed silanols.

those of the C_2H_4 complexes, so that the very weak manifestation of the ethylene π-complexes have a "transient" character. It is thus evident that, to clearly observe C_2H_4 molecular complexes under stationary conditions the polymerization must be avoided. Very recently some of us,[23] in a temperature-dependent FTIR experiment on a standard Cr(II)/SiO_2 sample, observed that a more precise detection of the C_2H_4 π-complexes is indeed possible when no polymerization has already occurred. We have applied a similar approach on the Cr(II)/SiO_2-aerogel system, focusing the attention on the 100−230 K temperature range, i.e., on the temperature range comprised between the ethylene melting point and the temperature at which the polymerization starts. The detection of the weak modes of coordinated ethylene has been facilitated by the use of the Cr/SiO_2-aerogel system, which allows to increase the number of Cr sites probed by the IR beam by more than 1 order of magnitude (see Introduction).

The spectrum of the Cr(II)/SiO_2-aerogel sample upon C_2H_4 adsorption at 120 K is reported in Figure 3, gray curve. At this temperature, besides the Cr(II)$\cdots(C_2H_4)_n$ complexes, ethylene physisorbed on the silica surface is highly contributing, as testified by the erosion of the silanol band at 3746 cm^{-1} and by the simultaneous growth of an intense band at about 3610 cm^{-1}, due to the OH vibration of the silanol groups in interaction with ethylene molecules (see left inset in Figure 3). If gaseous ethylene, due to its D_{2h} symmetry, presents two IR active C−H stretching modes, conversely, for a π-coordinated ethylene the symmetry is reduced, so that also the Raman active modes become IR visible and the ethylene mojety may have four active $\tilde{\nu}$(CH) bands in the IR spectrum. Indeed, in the CH_2 stretching region (gray spectrum in Figure 3), four main bands can be distinguished, at 3096 (vs), 3068 (m), 3006 (m) and 2978 (vs) cm^{-1}, easily assigned to the antisymmetric and symmetric CH_2 stretching modes of the physisorbed C_2H_4 molecules (see Table 1). The medium intensity bands correspond to the Raman active modes of gaseous ethylene, made IR active by reduction of symmetry. The adsorption makes also the $\tilde{\nu}$(C=C) stretching mode IR active (band at 1618 cm^{-1}, being the Raman band of

TABLE 1: Most Relevant Spectroscopic Features of C_2H_4 and $SiOH\cdots C_2H_4$ π-Complexes in the $\nu(CH_2)$, $\nu(C{=}C)$ and $\delta(CH_2)$ Regions[a]

	C_2H_4 (gas)	$SiOH\cdots C_2H_4$ π-complexes	
assignment	$\tilde{\nu}$ (cm^{-1})	$\tilde{\nu}$ (cm^{-1})	$\Delta\tilde{\nu}$ (cm^{-1})
$\nu_{as}(CH_2)$	3106 (IR)	3096 (vs)	-10
$\nu_{as}(CH_2)$	3103 (R)	3068 (m)	-35
$\nu s(CH_2)$	3026 (R)	3006 (m)	-20
$\nu_s(CH_2)$	2988 (IR)	2978 (vs)	-10
$\nu(C{=}C)$	1623 (R)	1618 (w)	-5
$\delta(CH_2)$	1444 (IR)	1440 (m)	-4

[a] For the π-complexes, the $\Delta\tilde{\nu}$ with respect to the gas phase are also reported. IR = IR active; R = Raman active. The intensity scale is as following: w = weak; m = medium; s = strong; vs = very strong.

the unperturbed molecule at 1623 cm^{-1}), as evident in the right inset of Figure 3, together with the intense band at 1440 cm^{-1}, due to the δ(CH) mode. Both the shift to low frequency of the silanol band at 3746 cm^{-1} and the perturbation of the vibrational modes of adsorbed ethylene can be explained on the basis of the formation of a 1:1 $SiOH\cdots C_2H_4$ π-complex. Formation of hydrogen-bonded ethylene π-complexes characterized by similar manifestations were previously reported for the acidic Brønsted sites of zeolites.[80] In the $\tilde{\nu}(C{=}C)$ stretching region, a second weaker component is observed at 1590 cm^{-1}, $\Delta\tilde{\nu}(C{=}C) = -33$ cm^{-1}. As this feature is absent in the same experiment performed on the bare silica surface, it is ascribed to $Cr(II)\cdots(C_2H_4)_n$ complexes. The intensity of the band at 1618 cm^{-1} is three times that of the 1590 cm^{-1} one, in fair agreement with the ratio of the surface abundances of silanols over Cr(II) species under the adopted activation conditions.[1,81]

With the only exception of the $\tilde{\nu}(C{=}C)$ stretching mode discussed above, at 120 K the spectrum is dominated by the features of $SiOH\cdots C_2H_4$ which overshadow the weaker manifestation of the significantly less abundant $Cr(II)\cdots(C_2H_4)_n$ complexes. However, as the adsorption enthalpy of the latter is much higher than that of the former, an increase of the temperature from 120 to 230 K (black thin curves in Figure 3) leads to the gradual disappearance of all the manifestations of the $SiOH\cdots C_2H_4$ complexes and to the gradual restoration of the unperturbed silanols (peak at 3746 cm^{-1}). In this way, the new, less intense bands associated with the C_2H_4 π-bonded to the Cr(II) sites become clearly visible (bold black line in Figure 3).

At 230 K the spectrum (bold black line in Figure 3) is only characterized by the features of the C_2H_4 π-complexes on the Cr(II) sites, i.e the spectrum does not present any component due to the ethylene in interaction with the silica surface (disappearance of the $\nu(C{=}C)$ band at 1618 cm^{-1}) and the polymerization reaction has not started at all. In the CH_2 stretching region five bands can be distinguished, at 3104 (w), 3084 (w), 3052 (vw), 3004 (m) and 2974 (vw) cm^{-1}. As for the case of $SiOH\cdots C_2H_4$ adducts, it is expected that the symmetry decrease induced by adsorption should allow the observation of four $\nu(CH_2)$ modes for the $Cr(II)\cdots(C_2H_4)_n$ complexes. While the bands at 3104, 3084, and 3004 cm^{-1} are plausibly assigned to the stretching modes of coordinated ethylene, the attribution of the 3052 and 2974 cm^{-1} bands is less certain. The spectrum of the $Cr(II)\cdots(C_2D_4)_n$ analogous system in the same experimental conditions is characterized by the presence of three bands in the CD_2 stretching region, at 2340 (w), 2317 (w) and 2245 (m) cm^{-1}, as reported in Figure 4b, black bold curve. The absence, in the spectrum of the $Cr(II)\cdots(C_2D_4)_n$ system, of the two bands analogous to the 3052 and 2974 cm^{-1} bands present in the case of the $Cr(II)\cdots(C_2H_4)_n$ system, suggests that these last ones may be due to the combination of low-frequency modes involving the $\tilde{\nu}(C{=}C)$ stretching, that is much less affected by isotopic substitution. In our opinion, only after a careful ab initio study of both $SiOH\cdots C_2H_4$ and $Cr(II)\cdots(C_2H_4)_n$ complexes, a safely full assignment is possible. The lower frequency region is characterized by the already discussed band at 1590 cm^{-1} of the IR activated $\tilde{\nu}(C{=}C)$ mode and by the 1444 cm^{-1} component of the δ(CH) mode. Bands similar to the two more intense ones (3004 and 1444 cm^{-1}) have been previously reported on standard $Cr(II)/SiO_2$ samples. In particular, Ghiotti et al.[15] observed two bands at 3006 and 1445 cm^{-1}, by performing the C_2H_4 polymerization reaction in the presence of CO acting as a poison (the shift in the ethylene frequencies being caused by the perturbation of CO), while Vikulov et al.[78] reported bands at 3000 and 1448 cm^{-1}, by injecting sequential small doses of ethylene into the cell. More recently, a "transient" band at 3004 cm^{-1} was assigned by Bade et al.[79] to an ethylene molecule coordinated to a Cr(II) site in a labile position, while Bordiga et al.,[23] by applying the same approach here presented on a standard $Cr(II)/SiO_2$ sample, were able to observe a band at 3005 cm^{-1}.

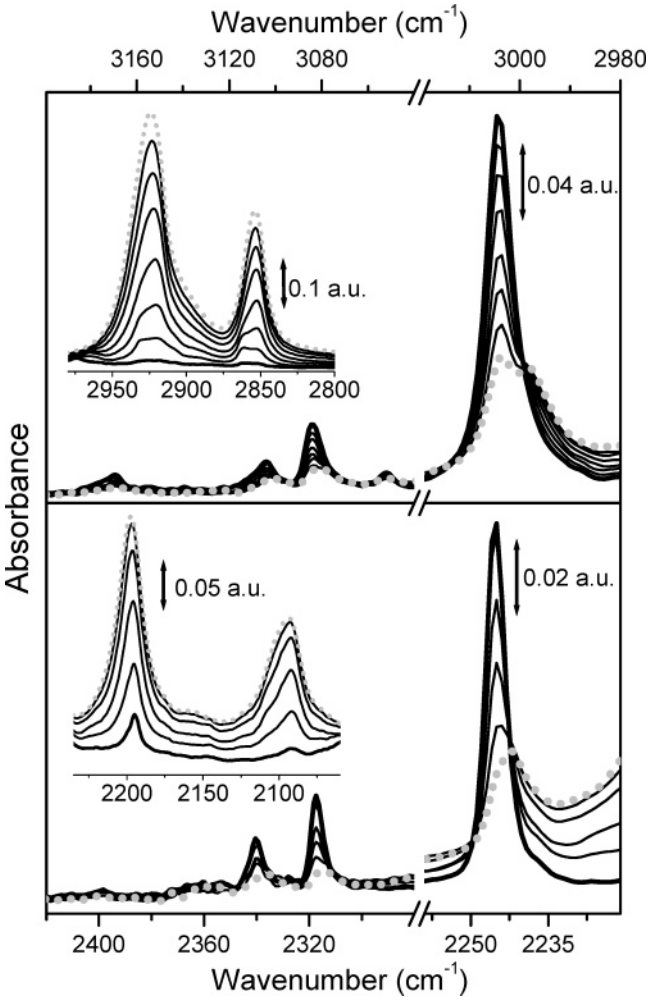

Figure 4. (a) Background subtracted temperature-resolved FTIR spectra, in the CH stretching region associated with the C_2H_4 π-bonded to Cr(II) sites, during the polymerization reaction in the 230−300 K range, from bold black to dotted gray curves. The black bold curve corresponds to the analogous reported in Figure 3. The inset reports, with the same color code, the bands due to the $\tilde{\nu}_{as}(CH_2)$ and $\tilde{\nu}_s(CH_2)$ modes of the living polymeric chains. (b) The same as panel a for C_2D_4.

When the temperature is allowed to grow from 230 K (bold black curve in Figure 4a) to 300 K (dotted gray curve in Figure 4a), the polymerization reaction slowly takes place, as evidenced by the appearance of two intense absorption bands around 2925 and 2855 cm^{-1}, due to the $\tilde{\nu}_{as}(CH_2)$ and $\tilde{\nu}_{s}(CH_2)$ modes of the living polymeric chains, as reported in the inset of Figure 4a (see Ref. 1). The two weak bands at 2931 and 2860 cm^{-1}, evident at short polymerization times, have been recently associated with some precursor species characterizing the polymerization reaction.[1,23] A detailed discussion of the assignment of these bands will be the topic of a successive work. Finally, note that the experiment here discussed is a temperature and pressure resolved experiment, i.e., the spectra are recorded at increasing temperature (from 230 to 300 K, from the bold to the dotted gray spectrum in Figure 4a) and at decreasing C_2H_4 pressure (due to the C_2H_4 consumption during the polymerization reaction). In the ethylene stretching region, reported in Figure 4a, we observe that the set of bands at 3104, 3084, and 3004 cm^{-1} already discussed begins to decrease when the monomer pressure declines (due to the polymerization process), evolving in a new set of bands at 3096, 3078 and 2998 cm^{-1}. The same behavior upon pressure decrease is followed also by the Cr(II)$\cdots(C_2D_4)_n$ system: in this case the set of bands at 2340, 2317 and 2245 cm^{-1} evolves into the new bands at 2336, 2313 and 2242 cm^{-1}, as reported in Figure 4b, accompanied by the growth of two intense bands at 2197 and 2094 cm^{-1}, due to the $\tilde{\nu}_{as}(CD_2)$ and $\tilde{\nu}_{s}(CD_2)$ modes of the living polymeric chains (see inset in Figure 4b).

Some of the bands related with the Cr(II)$\cdots(C_2H_4)_n$ complexes have been previously reported only by Bade et al.[79] and assigned to a "stable" ethylene−Cr complex, if compared with the "labile" one, responsible of the transient band at 3004 cm^{-1}. However, the evolution of the spectra as a function of the ethylene pressure reported in the present work (Figure 4), is suggesting another interpretation. We assign the set of bands at 3104, 3084, and 3004 cm^{-1} to the $\tilde{\nu}_{as}(CH_2)$ and $\tilde{\nu}_{s}(CH_2)$ modes of a di-ethylene π-bonded complex, which survives only until the monomer pressure is sufficiently high. Upon pressure decrease, this complex evolves into a mono-ethylene complex, characterized by the set of bands at 3096, 3078, and 2998 cm^{-1}. The experiments reported in Figure 4 are complex, on a thermodynamical ground, as both temperature and pressure contemporaneously change, see above. To separate the effect of pressure and temperature, an experiment performed at constant temperature should be ideal.[82] This experiment should give the same result of that discussed in the manuscript, but in a simpler situation, i.e., in absence of the polymerization reaction. Unfortunately, our experimental setup able to work at any defined temperature in the 12−300 K range[82] does not allow at the moment a complex activation procedure such as that required for the Cr/SiO_2 system (oxidation at high temperature and reduction in CO). We are trying to solve the experimental problems and we are looking forward for such an experiment in the future. However, when the experiment is performed in the presence of a high ethylene pressure (making the pressure drop negligible in first approximation, spectra not reported for brevity), the polymerization slowly takes place with increasing temperature, without affecting the set of bands at 3104, 3084 and 3004 cm^{-1}. This finally demonstrates our interpretation on the evolution of the bands shown in Figure 4a, and the fact that it is entirely due to the ethylene pressure decrease.

Unlike the case of H_2 and N_2, no distinction between the vibrational features of Cr(II)$\cdots C_2H_4$ complexes formed on different Cr(II) sites can be clearly observed, both for the di-ethylene and for the mono-ethylene π-bonded complexes. Finally, notwithstanding the fact that the Cr(II) sites on the silica surface have been found to be able to insert up to three molecules of CO and NO and to trimerize both acetylene and methylacetylene, (giving rise to benzene and 1,3,5-trimethylbenzene),[83] in the present work only mono and di-ethylene π-bonded complexes have been detected. However, the detection of an eventually present tri-ethylene complex could be extremely difficult due to the velocity of the following polymerization reaction.

4. Conclusions

In this work we report the first complete FTIR characterization of H_2 (and D_2,) N_2 and C_2H_4 (and C_2D_4) molecular adducts on the $Cr(II)/SiO_2$ system. The adoption of a silica aerogel as a support for the Cr(II) sites, being characterized by a higher surface area and by a lower scattering with respect to the common silica aerosil, allowed us to increase the number of Cr(II) sites crossed by the IR beam. In this way we have been able to detect the very weak vibrational manifestations of the molecular adducts formed on few Cr(II) sites, with a good signal-to-noise ratio. The evolution of the FTIR spectra as a function of the probe equilibrium pressure suggests that both H_2 and N_2 form, at low temperature, molecular complexes with two different types of Cr(II) sites, some of which are able to insert another probe molecule giving rise to Cr(II)$\cdots(H_2)_2$ or to Cr(II)$\cdots(N_2)_2$ complexes. Analogously, we observe the formation of di-ethylene π-bonded complexes, which survive only until the C_2H_4 pressure is sufficiently high, and which evolve in mono-ethylene complexes, when the C_2H_4 pressure decreases. The results here reported yield important information on the coordinative state of the Cr(II) ions, which well agrees with the evidences provided in the past by other probe molecules such as CO. Furthermore, the precise characterization of the π-bonded Cr(II)$\cdots(C_2H_4)_n$ complexes is the preliminary step in the attempt to solve the long standing question about the polymerization mechanism on the Phillips catalyst. In this work we move a first step along this direction.

References and Notes

(1) Groppo, E.; Lamberti, C.; Bordiga, S.; Spoto, G.; Zecchina, A. *Chem. Rev.* **2005**, *105*, 115−183 and references therein.
(2) Theopold, K. H. *Chemtech* **1997**, *27*, 26−32.
(3) Weckhuysen, B. M.; Schoonheydt, R. A. *Catal. Today* **1999**, *51*, 215−221.
(4) McDaniel, M. P. *Adv. Catal.* **1985**, *33*, 47−98.
(5) Zecchina, A.; Garrone, E.; Ghiotti, G.; Morterra, C.; Borello, E. *J. Phys. Chem.* **1975**, *79*, 966−972.
(6) Zecchina, A.; Garrone, E.; Morterra, C.; Coluccia, S. *J. Phys. Chem.* **1975**, *79*, 978−983.
(7) Zecchina, A.; Garrone, E.; Ghiotti, G.; Coluccia, S. *J. Phys. Chem.* **1975**, *79*, 972−978.
(8) Weckhuysen, B. M.; Schoonheydt, R. A.; Jehng, J. M.; Wachs, I. E.; Cho, S. J.; Ryoo, R.; Kijlstra, S.; Poels, E. *J. Chem. Soc., Faraday Trans.* **1995**, *91*, 3245−3253.
(9) Weckhuysen, B. M.; Wachs, I. E.; Shoonheydt, R. A. *Chem. Rev.* **1996**, *96*, 3327−3349.
(10) Rebenstorf, B.; Larsson, R. *Z. Anorg. Allg. Chem.* **1981**, *478*, 119−138.
(11) Ghiotti, G.; Garrone, E.; Della Gatta, G.; Fubini, B.; Giamello, E. *J. Catal.* **1983**, *80*, 249−262.
(12) Garrone, E.; Ghiotti, G.; Morterra, C.; Zecchina, A. *Z. Naturforsh. B* **1987**, *42*, 728−738.
(13) Ghiotti, G.; Garrone, E.; Zecchina, A. *J. Mol. Catal.* **1988**, *46*, 61−77.
(14) Rebenstorf, B. *J. Mol. Catal.* **1991**, *66*, 59−71.
(15) Ghiotti, G.; Garrone, E.; Zecchina, A. *J. Mol. Catal.* **1991**, *65*, 73−83.
(16) Garrone, E.; Abello, S.; Borello, E.; Ghiotti, G.; Zecchina, A. *Mater. Chem. Phys.* **1991**, *29*, 369−378.

(17) Spoto, G.; Bordiga, S.; Garrone, E.; Ghiotti, G.; Zecchina, A.; Petrini, G.; Leofanti, G. *J. Mol. Catal.* **1992**, *74*, 175−184.
(18) Zielinski, P.; Lana, I. G. D. *J. Catal.* **1992**, *137*, 368−376.
(19) Zielinski, P. A.; Szymura, J. A.; Lana, I. G. D. *Catal. Lett.* **1992**, *13*, 331−339.
(20) Kim, C. S.; Woo, S. I. *J. Mol. Catal.* **1992**, *73*, 249−263.
(21) Zecchina, A.; Spoto, G.; Ghiotti, G.; Garrone, E. *J. Mol. Catal.* **1994**, *86*, 423−446.
(22) Zecchina, A.; Scarano, D.; Bordiga, S.; Spoto, G.; Lamberti, C. *Adv. Catal.* **2001**, *46*, 265−397.
(23) Bordiga, S.; Bertarione, S.; Damin, A.; Prestipino, C.; Spoto, G.; Lamberti, C.; Zecchina, A. *J. Mol. Catal. A* **2003**, *204*, 527−534.
(24) Vuurman, M. A.; Wachs, I. E.; Stufkens, D. J.; Oskam, A. *J. Mol. Catal.* **1993**, *80*, 209−227.
(25) Dines, T. J.; Inglis, S. *Phys. Chem. Chem. Phys.* **2003**, *5*, 1320−1328.
(26) Groppo, E.; Damin, A.; Bonino, F.; Zecchina, A.; Bordiga, S.; Lamberti, C. *Chem. Mater.* **2005**, *17*, 2019−2027.
(27) Groppo, E.; Prestipino, C.; Cesano, F.; Bonino, F.; Bordiga, S.; Lamberti, C.; Thüne, P. C.; Niemantsverdriet, J. W.; Zecchina, A. *J. Catal.* **2005**, *230*, 98−108.
(28) Damin, A.; Bonino, F.; Bordiga, S.; Groppo, E.; Lamberti, C.; Zecchina, A., manuscript in preparation.
(29) Merryfield, R.; McDaniel, M. P.; Parks, G. *J. Catal.* **1982**, *77*, 348−359.
(30) van Kimmenade, E. M. E.; Kuiper, A. E. T.; Tamminga, Y.; Thune, P. C.; Niemantsverdriet, J. W. *J. Catal.* **2004**, *223*, 134−141.
(31) Gaspar, A. B.; Martins, R. L.; Schmal, M.; Dieguez, L. C. *J. Mol. Catal. A* **2001**, *169*, 105−112.
(32) Gaspar, A. B.; Brito, J. L. F.; Dieguez, L. C. *J. Mol. Catal. A* **2003**, *203*, 251−266.
(33) Lamberti, C.; Groppo, E.; Spoto, G.; Bordiga, S.; Zecchina, A. *Adv. Catal.* **2005**, invited review, submitted.
(34) http://www.novaratechnology.com/home.html.
(35) Kemper, P. R.; Bushnell, J. E.; Weis, P.; Bowers, M. T. *J. Am. Chem. Soc.* **1998**, *120*, 7577−7584.
(36) Aldridge, S.; Downs, A. J. *Chem. Rev.* **2001**, *101*, 3305−3365.
(37) Sweany, R. L.; Vuong, L.; Bishara, J. *J. Phys. Chem. A* **2002**, *106*, 11440−11445.
(38) Heidberg, J.; Vossberg, A.; Hustedt, M.; Thomas, M.; Briquez, S.; Picaud, S.; Girardet, C. *J. Chem. Phys.* **1999**, *110*, 2566−2578.
(39) Gribov, E. N.; Bertarione, S.; Scarano, D.; Lamberti, C.; Spoto, G.; Zecchina, A. *J. Phys. Chem. B* **2004**, *108*, 16174−16186.
(40) Kazansky, V. B. *J. Mol. Catal. A-Chem.* **1999**, *141*, 83−94.
(41) Stephanie-Victoire, F.; Cohen de Lara, E. *J. Chem. Phys.* **1998**, *109*, 6469−6475.
(42) Otero Areán, C.; Manoilova, O. V.; Bonelli, B.; Delgado, M. R.; Palomino, G. T.; Garrone, E. *Chem. Phys. Lett.* **2003**, *370*, 631−635.
(43) Zecchina, A.; Spoto, G.; Bordiga, S. *Phys. Chem. Chem. Phys.* **2005**, *7*, 1627−1642.
(44) Rosi, N. L.; Eckert, J.; Eddaoudi, M.; Vodak, D. T.; Kim, J.; O'Keeffe, M.; Yaghi, O. M. *Science* **2003**, *300*, 1127−1129.
(45) Zecchina, A.; Arean, C. O.; Palomino, G. T.; Geobaldo, F.; Lamberti, C.; Spoto, G.; Bordiga, S. *Phys. Chem. Chem. Phys.* **1999**, *1*, 1649−1657.
(46) Maseras, F.; Lledos, A.; Clot, E.; Eisenstein, O. *Chem. Rev.* **2000**, *100*, 601−636.
(47) Spoto, G.; Gribov, E.; Bordiga, S.; Lamberti, C.; Ricchiardi, G.; Scarano, D.; Zecchina, A. *Chem. Commun.* **2004**, 2768−2769.
(48) Kazansky, V. B.; Borovkov, V. Y.; Karge, H. G. *J. Chem. Soc., Faraday Trans.* **1997**, *93*, 1843−1848.
(49) Beck, K.; Pfeifer, H.; Staudte, B. *J. Chem. Soc., Faraday Trans.* **1993**, *89*, 3995−3998.
(50) Larin, A. V.; Cohen de Lara, E. *Mol. Phys.* **1996**, *88*, 1399−1410.
(51) Vitillo, J. G.; Damin, A.; Zecchina, A.; Ricchiardi, G. *J. Chem. Phys.* **2005**, *122*, Art. n. 114311 and references therein.
(52) Olkhov, R. V.; Nizkorodov, S. A.; Dopfer, O. *J. Chem. Phys.* **1997**, *107*, 8229−8238.
(53) Bushnell, J. E.; Kemper, P. R.; Bowers, M. T. *J. Phys. Chem.* **1994**, *98*, 2044−2049.
(54) Bordiga, S.; Garrone, E.; Lamberti, C.; Zecchina, A.; Otero Arean, C.; Kazansky, V. B.; Kustov, L. M. *J. Chem. Soc., Faraday Trans.* **1994**, *90*, 3367−3372.
(55) Senchenya, I. N.; Kazanskii, V. B. *Kinet. Katal.* **1988**, *29*, 1131.
(56) Solans-Monfort, X.; Branchadell, V.; Sodupe, M.; Zicovich-Wilson, C. M.; Gribov, E.; Spoto, G.; Busco, C.; Ugliengo, P. *J. Phys. Chem. B* **2004**, *108*, 8278−8286.
(57) Amor Nait Ajjou, J.; Scott, S. L. *J. Am. Chem. Soc.* **2000**, *122*, 8968−8976.
(58) Sellmann, D. *Angew. Chem., Int. Ed. Engl.* **1974**, *13*, 639.
(59) Pelikan, P.; Boca, R. *Coord. Chem. Rev.* **1984**, *55*, 55−112.
(60) Chang, C. C.; Kokes, R. J. *J. Phys. Chem.* **1973**, *77*, 49−62.
(61) Egerton, T. A.; Sheppard, N. *J. Chem. Soc., Faraday Trans.* **1974**, *70*, 1357−1365.
(62) Kuroda, Y.; Konno, S.; Morimoto, K.; Yoshikawa, Y. *J. Chem. Soc.-Chem. Commun.* **1993**, 18−20.
(63) Miessner, H. *J. Am. Chem. Soc.* **1994**, *116*, 11522−11530.
(64) Spoto, G.; Bordiga, S.; Ricchiardi, G.; Scarano, D.; Zecchina, A.; Geobaldo, F. *J. Chem. Soc., Faraday Trans.* **1995**, *91*, 3285−3290.
(65) Geobaldo, F.; Lamberti, C.; Ricchiardi, G.; Bordiga, S.; Zecchina, A.; Palomino, G. T.; Arean, C. O. *J. Phys. Chem.* **1995**, *99*, 11167−11177.
(66) Lamberti, C.; Bordiga, S.; Salvalaggio, M.; Spoto, G.; Zecchina, A.; Geobaldo, F.; Vlaic, G.; Bellatreccia, M. *J. Phys. Chem.* **1997**, *101*, 344−360.
(67) Kuroda, Y.; Maeda, H.; Yoshikawa, Y.; Kumashiro, R.; Nagao, M. *J. Phys. Chem. B* **1997**, *101*, 1312−1316.
(68) Miessner, H.; Richter, K. *J. Mol. Catal. A-Chem.* **1999**, *146*, 107−115.
(69) Rest, A. J. *J. Organomet. Chem.* **1972**, *40*, C76.
(70) Huber, H.; Kunding, E. P.; Moskovits, M.; Ozin, G. A. *J. Am. Chem. Soc.* **1973**, *95*, 332−344.
(71) Chatt, J.; Ducanson, L. A.; Guy, R. G. *Nature* **1959**, *184*, 526.
(72) Heberhold, M. *Metal π-Complexes: Vol. II, Complexes with Mono-Olefinic Ligands*; Elsevier: Amsterdam, 1974.
(73) Huber, H.; Ozin, G. A.; Power, W. J. *J. Am. Chem. Soc.* **1976**, *98*, 6508−6511.
(74) Merlemejean, T.; Cossemertens, C.; Bouchareb, S.; Galan, F.; Mascetti, J.; Tranquille, M. *J. Phys. Chem.* **1992**, *96*, 9148−9158.
(75) Vikulov, K. A.; Elev, I. V.; Shelimov, B. N.; Kazansky, V. B. *J. Mol. Catal.* **1989**, *55*, 126−145.
(76) Vikulov, K. A.; Shelimov, B. N.; Kazansky, V. B. *J. Mol. Catal.* **1991**, *65*, 393−402.
(77) Alexander, B. D.; Dines, T. J. *J. Phys. Chem. A* **2004**, *108*, 146−156.
(78) Vikulov, K.; Spoto, G.; Coluccia, S.; Zecchina, A. *Catal. Lett.* **1992**, *16*, 117−122.
(79) Bade, O. M.; Blom, R.; Dahl, I. M.; Karlsson, A. *J. Catal.* **1998**, *173*, 460−469.
(80) Spoto, G.; Bordiga, S.; Ricchiardi, G.; Scarano, D.; Zecchina, A.; Borello, E. *J. Chem. Soc., Faraday Trans.* **1994**, *90*, 2827−2835.
(81) Zhuravlev, L. T. *Colloid Surf. A* **2000**, *173*, 1−38.
(82) Spoto, G.; Gribov, E. N.; Ricchiardi, G.; Damin, A.; Scarano, D.; Bordiga, S.; Lamberti, C.; Zecchina, A. *Prog. Surf. Sci.* **2004**, *76*, 71−146.
(83) Zecchina, A.; Bertarione, S.; Damin, A.; Scarano, D.; Lamberti, C.; Prestipino, C.; Spoto, G.; Bordiga, S. *Phys. Chem. Chem. Phys.* **2003**, *5*, 4414−4417.